



## Modelling the Transition of Asexual Blood Stages of *Plasmodium falciparum* to Gametocytes

HANS H. DIEBNER\*†, MARTIN EICHNER\*, LOUIS MOLINEAUX‡§,  
WILLIAM E. COLLINS¶, GEOFFREY M. JEFFERY¶§ AND KLAUS DIETZ\*

\*Department of Medical Biometry, University of Tübingen, Westbahnhofstr. 55, D-72070 Tübingen, Germany, †World Health Organisation and ‡Centers for Disease Control and Prevention, U.S. Public Health Service, Department of Health and Human Services, Atlanta, GA, U.S.A.

(Received on 4 May 1999, Accepted in revised form on 21 October 1999)

In this paper, we investigate the transition of asexual blood stages of *P. falciparum* to gametocytes. The study is based on daily data, collected from 262 individual courses of parasitaemia. We propose several mathematical models that follow biological reasoning. The models are fitted with maximum likelihood and are compared with each other. The models differ in the assumptions made about the mortality of circulating gametocytes and about the transition rate of the asexual parasites. Gametocyte mortality is modelled as being (i) constant over time, (ii) linearly increasing over time, (iii) linearly increasing over gametocyte age, and (iv) exponentially increasing over gametocyte age, respectively. The transition rate is either kept constant per patient or piecewise constant within intervals that correspond to waves of asexual parasitaemia which are assumed to be caused by different  $Pf_{emp1}$ -variants. According to likelihood ratio tests, the models with age-dependent mortality rate and wave-dependent transition rates are superior to the models with constant transition rate and/or constant or time-dependent mortality rate. The best fits are reached for models with exponentially increasing (Gompertz-type) mortality. Furthermore, an impact of high asexual parasite densities on the survival of gametocytes, interpreted as a cytokine-mediated effect, is evident in some cases.

© 2000 Academic Press

### 1. Introduction

In terms of morbidity, the sexual stages of *Plasmodium falciparum* and other malaria parasites probably play only a minor role although an essential one in terms of the parasite's transmission, as only they can infect mosquitoes. Therefore, a realistic model for the generation and persistence of the sexual stages of *P. falciparum* detectable in the human blood, i.e. the *P.*

*falciparum* gametocytes, would be relevant for malaria control. Each cycle of erythrocytic schizogony, i.e. of multiplication within human red blood cells (RBC), lasts about 48 h, at the end of which the parasitized red blood cell (PRBC) bursts, liberating on average 16 merozoites. A successful merozoite invades another RBC within minutes and takes one of two routes: it either goes into another round of schizogony or develops into a single gametocyte, male or female. Commitment to gametocytogenesis is presumably made during the immediately preceding cycle of schizogony. Newly invaded RBCs of

† Author to whom correspondence should be addressed.  
E-mail: [hd@zkm.de](mailto:hd@zkm.de)  
§ Retired.

both kinds circulate for about a day, then sequester for either a day until rupture and release of new merozoites, or for the period it takes for gametocyte maturation. Mature gametocytes are released into the circulation, where they are detectable by standard microscopy, and can be picked up by an anopheline vector, in the midgut of which gametocytes develop into gametes and fertilization allows the life cycle to continue. Commonly available parasitologic examinations, including those used to produce our data, are not able to distinguish between rings which are committed to become gametocytes and others which will develop into schizonts, nor between male and female gametocytes (Bruce *et al.*, 1990; Carter & Graves, 1988; Carter & Miller, 1979; Day *et al.*, 1998; Garnham, 1988).

Gametocytogenesis has been studied extensively *in vitro* for different biological purposes, not necessarily relevant for gametocytogenesis *in vivo*. Of potential though questionable relevance may be the marked and rapid increase in gametocytogenesis associated with increasing parasite density, and its marked and rapid decrease associated with dilution with fresh RBCs (Carter & Miller, 1979; Bruce *et al.*, 1990). With respect to gametocyte survival, it has been shown for *P. cynomolgi*, *p. vivax* and *P. falciparum* that, in non-immunes, a parasite-mediated release of cytokines, commonly associated with high asexual stage densities, increases gametocyte mortality (Naotunne *et al.*, 1991, 1993; Karunaweera *et al.*, 1992). At least in the case of *P. vivax*, acquired anti-disease immunity neutralizes this effect (Karunaweera *et al.*, 1992). With respect to acquired immunity against *P. falciparum*, a positive effect on gametocytogenesis has been observed *in vitro* (Smalley & Brown, 1981), but a negative gametocytaemia, in excess of the effect on asexual parasitaemia, has been observed *in vivo*, perhaps explained by an antibody-mediated increase in gametocyte mortality (Baird *et al.*, 1991).

The purpose of this paper is to describe different models, predicting gametocytaemia from asexual parasitaemia, and the process by which they were fitted to the data and compared to each other. In Section 2, we describe the data. In Section 3, we formulate different model assumptions and incorporate them into increasingly

complex models. In Section 4, we describe how the models are fitted to individual case histories. In Section 5, we compare the fits of the different models and identify the model which in general yields the most satisfactory fit to the data. In Section 6, we outline some previously published models, present a summary of our parameter estimates and discuss some unsatisfactory fits. A detailed discussion of the parameter estimates, obtained with the best model, and their biological implications will be presented elsewhere.

## 2. The Data

Malariatherapy data have made a major contribution to our knowledge of patterns of asexual parasitaemia, gametocytaemia and infectivity to the vector, for different species of human malaria parasites, including *P. falciparum*. The data used here were collected by the USPHS in the NIH Laboratories in Columbia, SC, and Milledgeville, GA, at a time when malariatherapy was a recommended treatment of neurosyphilis. Detailed descriptions of the available data have been given in numerous previous publications (Eyles & Young, 1951; Jeffery & Eyles, 1954; Jeffery, 1960). The parasite of choice was *P. vivax*, to which Afroamericans were however found to be refractory, and so they were treated with different strains of *P. falciparum* under close medical supervision. They were inoculated either with sporozoites (generally through mosquito bite) or with infected blood. Inoculations were preceded by variable sequences of blood and mosquito passages of the strain. Microscopic examination of the blood was performed on an almost daily basis. In principle, 0.1  $\mu\text{l}$  of blood was examined, less in case of high densities, occasionally more; the detection threshold was thus about 10 PRBC/ $\mu\text{l}$  (Earle & Perez, 1932). Two classes of PRBC were counted separately: "asexual parasites" (including immature gametocytes less than one day old) and "gametocytes" (i.e. mature gametocytes of unknown sex). Usually, gametocyte stage densities were reported as ten-fold of the actual counts. This fact was taken into account in the analysis. The data which were evaluated in this study concern only primary *P. falciparum* inoculations and, among those, only cases with at least four positive gametocyte observations.

### 3. Hierarchy of Models

In order to describe the dynamics of gametocytaemia, it is necessary to make assumptions concerning the transition of asexual parasites to gametocytes, the sequestration time and the survival of gametocytes. The biological literature reports relevant observations and hypotheses, but is not very conclusive (Carter & Graves, 1988). With respect to gametocytogenesis, the simplest assumption is that a constant proportion of asexual parasites convert to gametocytes within each cycle. Indeed, at first glance, the parasitaemia of several patients conveys the impression that waves of asexual parasites are followed by waves of gametocytes in which the latter are displaced by some days—the sequestration phase—and have lower amplitudes (see Figs 2–5). Assuming a constant conversion probability of asexual parasites into circulating gametocytes as well as a constant force of gametocyte mortality, one expects a constant ratio of the area under the gametocyte curve to the area under the asexual curve, but a closer look at the curves suggests that the ratio of the two areas varies among waves. There are indications that the observed waves of asexual parasitaemia reflect the development of different intraclonal variants of the parasite molecule  $Pf_{emp1}$ , expressed on the surface of PRBCs, corresponding to different cytoadherence phenotypes and responsible for sequestration of asexual parasites (Borst *et al.*, 1995). Furthermore, the same molecule is involved in the sequestration of gametocytes and its expression has been shown to be genetically linked with gametocytogenesis on the parasite's chromosome 9 (Day *et al.*, 1998). Thus, it seems justified to vary the conversion probability among asexual waves.

Based on inspection of the data and on the suggestions from the biological literature, we formulated different models and fitted them to individual case histories, thus obtaining case-specific parameter estimates. All our models predict the number of mature gametocytes entering the circulation at time  $t$  from the reported number of “asexual” parasites at time  $t - D_s$ , where  $D_s$  is the sequestration time which is needed for gametocyte maturation. The different models are defined by the following options: (i) the

probability of successful gametocytogenesis (i.e. the product of the conversion probability and the probability to survive the sequestration period) is either constant for the patient or step-wise constant for each wave of asexual parasites; (ii) the mortality rate of circulating gametocytes is either constant or it increases over time or gametocyte age; (iii) additional gametocyte mortality may be caused by the presence of asexual parasites. We present combinations of options as a branching hierarchy of models.

The basic structure of all proposed models can be described as follows. Circulating asexual parasites  $A(t)$  on day  $t$  convert to sequestered gametocytes at rate  $\gamma(t)$ . After time delay  $D_s$ , sequestered gametocytes enter the circulating blood and from then on can be detected via microscopic blood examination. The circulating gametocytes,  $G(t)$ , die at rate  $\mu(t)$ . This leads to the delay equation

$$\frac{dG(t)}{dt} = \gamma(t - D_s)A(t - D_s) - \mu(t)G(t). \quad (1)$$

The examined family of models makes different assumptions concerning the conversion rate  $\gamma(t)$  and the mortality rate  $\mu(t)$ . The model hierarchy is schematically depicted in Fig. 1 and a compilation of all proposed models is given in Table 1.

The most basic model assumes that  $\gamma$  and  $\mu$  are constant. The solution of eqn (1) for this case is

$$G(t) = \gamma \int_{D_s}^t A(\tau - D_s) e^{-(t-\tau)\mu} d\tau. \quad (2)$$

In the parameter estimation routine, we use the discretized approximation

$$G(t) = \gamma \sum_{\tau=D_s+1}^t A(\tau - D_s) e^{-(t-\tau)\mu} \quad (3)$$

as the prediction formula because we have only one data point for each day. Asexual parasites circulate for one day only, so that the product  $\gamma$  times one day may be interpreted as transition probability. Maximum likelihood estimates of the parameters  $\mu$ ,  $\gamma$  and  $D_s$  are calculated as described in Section 3. To motivate the following extensions of the basic model, we anticipate some

of the results by referring to Figs 2–4 (a detailed model comparison will be performed in Section 4). The figures show the observed asexual parasitaemia and gametocytaemia of three arbitrarily selected patients and their gametocytaemia, as

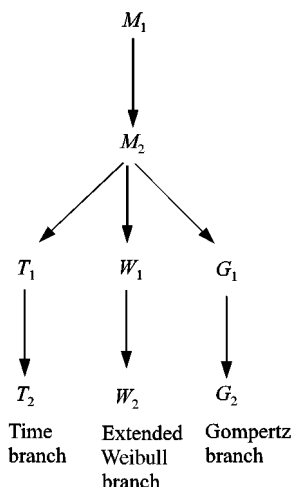


FIG. 1. Hierarchical model structure.  $M_1$  denotes the basic model with constant transition rate  $\gamma$  from asexual stages to gametocytes and constant gametocyte mortality rate  $\mu$ . In  $M_2$ , the mortality is still constant, but—as in all higher models—the transition rates  $\gamma$  differ between asexual waves. There is a bifurcation in the model hierarchy leading to three model branches: (1) in models  $T_1$  and  $T_2$ , we assume that mortality increases linearly with time; (2) in models  $W_1$  and  $W_2$ , we assume that mortality increases linearly with the age of the gametocytes (Weibull-type mortality); (3) in models  $G_1$  and  $G_2$ , we assume that mortality increases exponentially with the age of the gametocytes (Gompertz-type mortality). The models of highest complexity ( $T_2$ ,  $W_2$  and  $G_2$ ) furthermore include the feature of “cytokine-mediated” gametocyte mortality produced by asexual parasites (see text for details).

predicted by the proposed models. Note that in all figures one parasite is added to each observed or predicted value in order to depict zero observations on a logarithmic scale. The dotted lines (marked  $M_1$ ) show results of the basic model as described above. The basic model fails to fit the data well. The amplitudes of the expected curves ( $M_1$ ) indicate that the basic model mainly fails because the various waves of the asexual parasitaemia produce gametocytes at different rates, whereas for most patients with a single asexual wave, constant  $\mu$  and  $\gamma$  are sufficient (data not shown).

We now introduce a piecewise constant  $\gamma$  by assigning to each wave of asexual parasitaemia a different value of  $\gamma$ . In order to structure the asexual parasitaemia in waves, we first identify peaks: a parasite density  $A(t)$  at time  $t$  is called a peak if

$$A(t - \tau) < A(t) \geq A(t + \tau), \quad \tau = 1, 2, \dots, 6. \quad (4)$$

For each peak there is exactly one wave of asexual parasitaemia which ends halfway between two subsequent peaks. Some results of the extended model are shown in Figs 2–4, marked  $M_2$ . Waves of asexual parasites lead to waves of gametocytes which approximately match the observations. The arrows on the upper margins of the plots designate the peaks. The estimates of consecutive  $\gamma$  vary in a non-systematic manner and exhibit no clear tendency.

We now allow for possible effects of immunity by incorporating a gametocyte mortality which

TABLE 1  
*Model compilation: the models differ in gametocyte production and in the gametocyte mortality*

Model	Transition rate to gametocytes	Mortality rate
$M_1$	$\gamma = \text{const}$	$\mu(t) = \mu_0$
$M_2$	$\gamma = \gamma(\text{wave})$	$\mu(t) = \mu_0$
$T_1$	$\gamma = \gamma(\text{wave})$	$\mu(t) = \mu_0 + \alpha_T t$
$T_2$	$\gamma = \gamma(\text{wave})$	$\mu(t) = \mu_0 + \alpha_T t + \beta \log_{10}(A(t) + 1)$
$W_1$	$\gamma = \gamma(\text{wave})$	$\mu(t, a) = \mu_0 + \alpha_w a$
$W_2$	$\gamma = \gamma(\text{wave})$	$\mu(t, a) = \mu_0 + \alpha_w a + \beta \log_{10}(A(t) + 1)$
$G_1$	$\gamma = \gamma(\text{wave})$	$\mu(t, a) = \mu_0 e^{\alpha_a a}$
$G_2$	$\gamma = \gamma(\text{wave})$	$\mu(t, a) = \mu_0 e^{\alpha_a a} + \beta \log_{10}(A(t) + 1)$

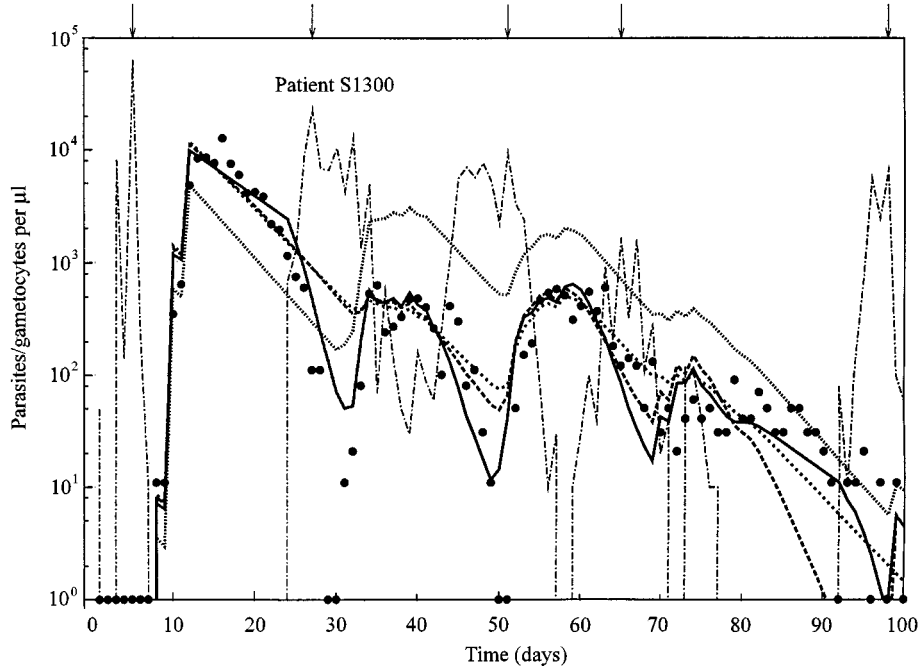


FIG. 2. Comparison of the observed and expected gametocytaemia as predicted by models  $M_1$ ,  $M_2$ ,  $T_1$  and  $T_2$ , (see Table 5 for parameter estimates).  $M_1$ : constant mortality and transition rates.  $M_2$ : constant mortality rate; this and all further models assume different transition rates for each asexual wave.  $T_1$ : mortality rate grows linearly with time.  $T_2$ : like  $T_1$ , but with additional cytokine-mediated mortality (see text for details). The asexual parasitaemia is used as input function from which the gametocytaemia is calculated. Maxima which define asexual waves are marked with arrows at the upper margin: (-----) asexual parasites; (●) observed gametocytes; (.....)  $M_1$ ; (---)  $M_2$ ; (----)  $T_1$ ; (—)  $T_2$ .

grows over time, i.e.

$$\mu(t) = \mu_0 + \alpha_T t. \quad (5)$$

This leads to the following discretized approximation of  $G(t)$  which is used as the prediction formula in the parameter estimation routine of model  $T_1$ :

$$G(t) = \sum_{\tau=D_s+1}^t \gamma(\tau - D_s) A(\tau - D_s) \times \exp\left(-\mu_0(t - \tau) - \frac{\alpha_T}{2}(t^2 - \tau^2)\right). \quad (6)$$

The results fit better to the data than in the previous models (see Fig. 2, dashed line, marked  $T_1$ ), but dips in the observed gametocytaemia which seem to coincide with asexual peaks are frequently missed.

Following the argument that gametocyte mortality may be influenced by cytokines which are

released when RBCs rupture (Naotunne *et al.*, 1991, 1993; Karunaweera *et al.*, 1992), we incorporate an additional mortality term into the model which depends on the logarithm of the density of asexual parasites:

$$\mu(t) = \mu_0 + \alpha_T t + \beta \log_{10}(A(t) + 1). \quad (7)$$

This leads to the following discretized approximation of  $G(t)$  which is used as the prediction formula in the parameter estimation routine of model  $T_2$ :

$$G(t) = \sum_{\tau=D_s+1}^t \gamma(\tau - D_s) A(\tau - D_s) \times \exp\left(-\mu_0(t - \tau) - \alpha_T(t^2 - \tau^2) - \beta \sum_{s=\tau}^t \log_{10}(A(s) + 1)\right). \quad (8)$$

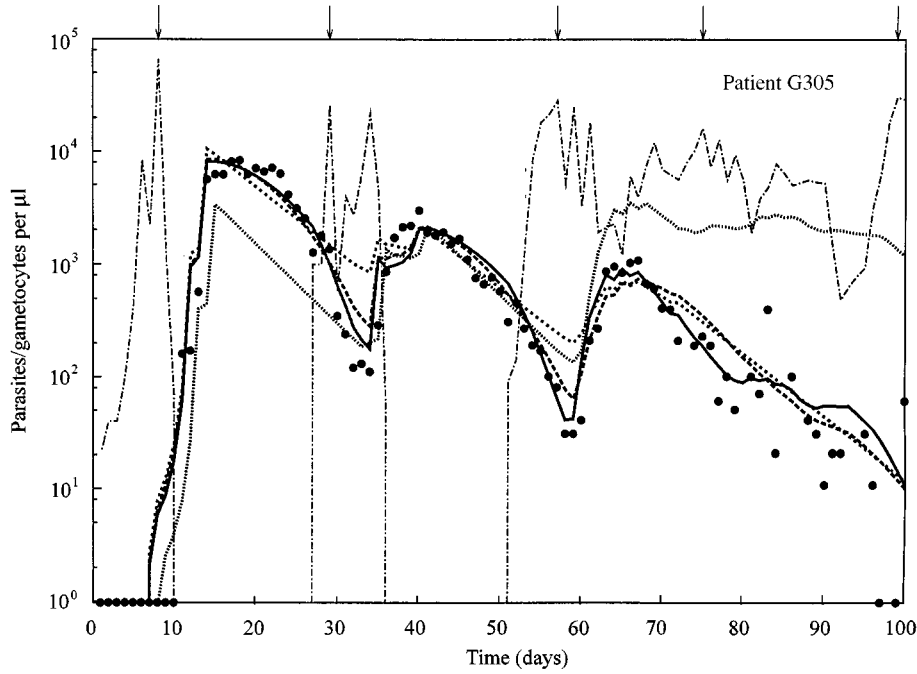


FIG. 3. Comparison of the observed and expected gametocytaemia as predicted by models  $M_1$ ,  $M_2$ ,  $W_1$  and  $W_2$ , respectively (see Table 5 for parameter estimates).  $M_1$ : constant mortality and transition rates.  $M_2$ : constant mortality rate; this and all further models assume different transition rates for each asexual wave.  $W_1$ : mortality rate grows linearly with the age of the gametocytes (Weibull-type mortality).  $W_2$ : like  $W_1$ , but with additional cytokine-mediated mortality (see text for details). The asexual parasitaemia is used as input function from which the gametocytaemia is calculated. Maxima which define asexual waves are marked with arrows at the upper margin: (---) asexual parasites; (●) observed gametocytes; (.....)  $M_1$ ; (-.-.-)  $M_2$ ; (- - -)  $W_1$ ; (—)  $W_2$ .

Dips are often much better reproduced than in the previous models (Fig. 2; line marked  $T_2$ ), but many fits are still not fully satisfactory.

Gametocyte mortality may depend on the age of the individual gametocyte rather than on the immune status (represented by the time since onset of patency) during the first parasitaemia of a patient. Such age-dependent mortality is seen in many species, whereby the Weibull and the Gompertz distributions often provide satisfactory models. In order to incorporate the age  $a$  of gametocytes into the model, the dynamics have to be described by a partial differential equation

$$\frac{\partial g(t, a)}{\partial t} + \frac{\partial g(t, a)}{\partial a} = -\mu(t, a)g(t, a), \quad (9)$$

$$g(t, 0) = \gamma(t - D_s)A(t - D_s), \quad (10)$$

where  $g(t, a)$  is the probability density of gametocytes which depends on time  $t$  since the onset of patency and on age  $a$  of the gametocytes.

The force of mortality  $\mu(t, a)$  according to Weibull is proportional to  $a^\delta$ . We choose  $\delta = 1$  and extend the formula by adding a constant term  $\mu_0$ , i.e. we assume that the mortality increases linearly with age:

$$\mu(a, t) = (\mu_0 + \alpha_w a) + \beta \log_{10}(A(t) + 1). \quad (11)$$

Incorporating this expression into eqn (9) leads to the following discretized approximation of  $G(t)$  which is used as the prediction formula in the parameter estimation routines of models  $W_1$  and  $W_2$ :

$$G(t) = \sum_{\tau=D_s+1}^t \gamma(\tau - D_s)A(\tau - D_s) \times \exp\left(-\mu_0(t - \tau) - \frac{\alpha_w}{2}(t^2 - \tau^2) - \beta \sum_{s=\tau}^t \log_{10}(A(s) + 1)\right). \quad (12)$$

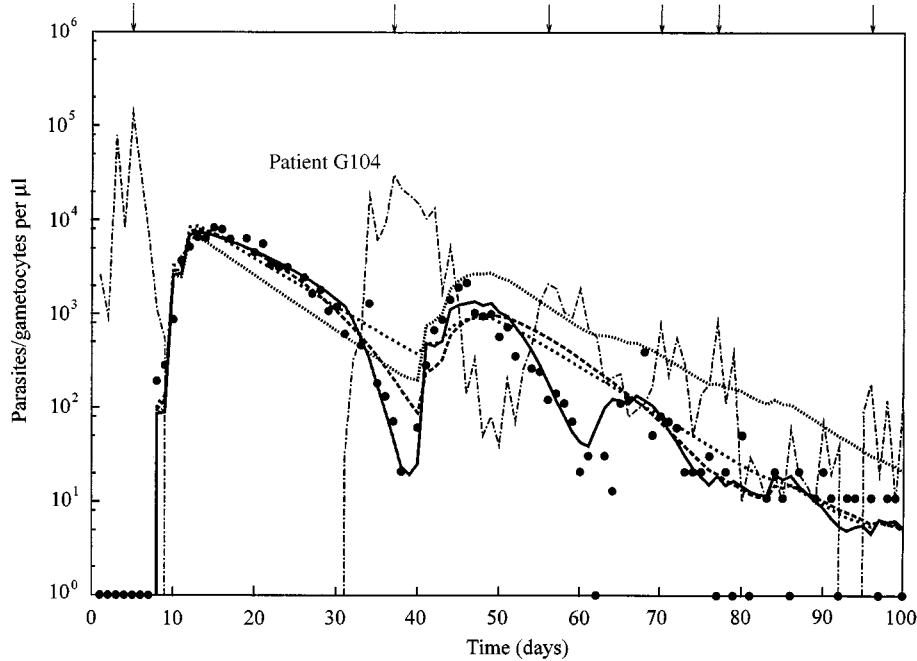


FIG. 4. Comparison of the observed and expected gametocytaemia as predicted by models  $M_1$ ,  $M_2$ ,  $G_1$  and  $G_2$ , respectively (see Table 5 for parameter estimates).  $M_1$ : constant mortality and transition rates.  $M_2$ : constant mortality rate; this and all further models assume different transition rates for each asexual wave.  $G_1$ : mortality rate grows exponentially with the age of the gametocytes (Gompertz-type mortality).  $G_2$ : like  $G_1$ , but with additional cytokine-mediated mortality (see text for details). The asexual parasitaemia is used as input function from which the gametocytaemia is calculated. Maxima which define asexual waves are marked with arrows at the upper margin: (---) asexual parasites; (●) observed gametocytes; (.....)  $M_1$ ; (.....)  $M_2$ ; (---)  $G_1$ ; (—)  $G_2$ .

Results are shown in Fig. 3 for  $\beta = 0$  (model  $W_1$ ) and for estimated  $\beta$  (model  $W_2$ ). Compared to the results of models  $M_1$  and  $M_2$ , the improvements are obvious.

As an alternative to the Weibull approach, we may assume that gametocyte mortality increases exponentially with age as predicted by the Gompertz mortality model:

$$\mu(t, a) = \mu_0 e^{\alpha a} + \beta \log_{10}(A(t) + 1). \quad (13)$$

Incorporating this expression into eqn (9) leads to the following discretized approximation of  $G(t)$  which is used as the prediction formula in the parameter estimation routines of models  $G_1$  and  $G_2$ :

$$G(t) = \sum_{\tau=D_s+1}^t \gamma(\tau - D_s) A(\tau - D_s) \times \exp\left(-\frac{\mu_0}{\alpha_G} (e^{\alpha_G(t-\tau)} - 1) - \beta \sum_{s=\tau}^t \log_{10}(A(s) + 1)\right). \quad (14)$$

Results of the proposed model are shown in Fig. 4 for  $\beta = 0$  (model  $G_1$ ) and for estimated  $\beta$  (model  $G_2$ ). The exponentially increasing mortality leads to a more abrupt decline of the gametocyte waves. Qualitative judgement of graph  $G_1$  already turns out to be quite satisfactory, but the dips at the days 38 and 62 are fitted much better by  $G_2$ .

#### 4. Fitting the Models to Individual Case Histories

A separate set of parameters was estimated for each individual patient using a maximum likelihood procedure for which we assume that the reported gametocyte stage densities per 0.1  $\mu\text{l}$  blood are Poisson distributed. The expected time series of gametocytes are calculated with the prediction formulas of models  $M_1$  through  $G_2$  (cf. Table 1 for a model compilation), using the reported densities of asexual parasites per 0.1  $\mu\text{l}$  as input. We fitted the course of parasitaemia up to day 100 for each individual (unless it ended earlier). Parasitaemias following day 100 often

consisted of isolated observations of low density, separated by large intervals of zeros. Our definition of waves would lead to many additional  $\gamma$ -parameters which may not reliably be estimated from such sparse data. A 100-day fit turned out to be a good compromise between completeness and the capability of finding reliable parameter values. Unfortunately, data on asexual parasites and on gametocytes are missing for several days, but our formulas can only be evaluated for a complete time series of asexual parasites. Missing asexual observations are, therefore, interpolated with a linear function. For days with missing gametocyte observations, no comparison between observed and expected values is possible and the contribution to the likelihood is set equal to one.

As the estimation procedure frequently converged to local maxima, many runs were needed for each patient before one could be sure to have reached the global maximum. We performed up to hundreds of repetitions, partially choosing initial parameter values at random and partly starting with parameter values which yielded the best likelihood so far. The rather flat shape of the log-likelihood may at least partly be caused by relatively strong correlations of parameters, especially between transition rate and mortality rate. A further problem concerns the estimation of sequestration time  $D_s$ . Being an integer,  $D_s$  cannot be estimated in a continuous maximization procedure. Several maximization runs with fixed values of  $D_s$  were performed and the value leading to the largest likelihood for the patient was chosen.

### 5. Comparison of Models

A first quick model comparison can be made by comparing the sums of the log-likelihoods of all 262 patients for the different models. The models  $T_1$  (time-dependent mortality),  $W_1$  (Weibull mortality) and  $G_1$  (Gompertz mortality) have the same number of parameters and cannot formally be compared using likelihood ratio tests. The difference of the log-likelihood sums between  $T_1$  and  $W_1$  equals 3913, indicating that the assumption of Weibull mortality provided better fits than that of time-dependent mortality. The difference between  $G_1$  and  $W_1$  equals

1054, indicating that the model with Gompertz mortality fitted the data even better than that with Weibull mortality. The same holds for the models with additional cytokine-mediated mortality: the difference between  $W_2$  and  $T_2$  equals 4661 and the difference between  $G_2$  and  $W_2$  equals 1253, again indicating that the data are best fitted by using Gompertz mortality.

The model sequence  $M_1$ - $M_2$ - $T_1$ - $T_2$  is hierarchically structured and, therefore, allows comparisons with the likelihood ratio test. Forty out of 262 cases have only one wave of asexual parasitaemia, i.e. models  $M_1$  and  $M_2$  are identical. For 198 out of the remaining 222 cases, model  $M_2$  leads to significantly better fits than  $M_1$  ( $p \leq 0.05$ ). Table 2 shows how the numbers of cases where  $M_2$  leads to significantly better fits depends on the number of asexual waves (i.e. the number of different  $\gamma$ -estimates). Twelve out of the 24 cases without significant improvement show parasite courses which consist of only two waves. A total of 129 fits is significantly improved when going from model  $M_2$  to  $T_1$  (Table 2), i.e. almost half of all cases are fitted better when changing from a constant force of mortality to a linearly increasing one. A monotonous trend of the proportion of significant improvements depending on the number of waves cannot be confirmed ( $p = 0.38$ ; logistic regression). A total of 86 cases is significantly improved when going from model  $T_1$  to  $T_2$  (Table 2). The probability that adding cytokine-mediated mortality leads to a significant improvement of the fit grows with the number of asexual waves per patient ( $p = 0.004$ ; logistic regression).

A second branch of hierarchically structured models is given by the sequence  $M_1$ - $M_2$ - $W_1$ - $W_2$ . Going from  $M_2$  to  $W_1$ , i.e. using age-dependent (Weibull) mortality instead of constant  $\mu$  leads to 73 significantly improved fits (Table 2) whereby the proportion of significant improvements slightly increases with the number of asexual waves ( $p = 0.04$ ; logistic regression). Adding cytokine-mediated mortality (model  $M_2$ ) leads to 76 significant improvements compared to  $M_1$ , but a dependency on the number of waves cannot be confirmed for this model ( $p = 0.11$ ; logistic regression).

Finally, the sequence  $M_1$ - $M_2$ - $G_1$ - $G_2$  is hierarchically structured. Model  $G_1$  yields 82

TABLE 2

*Model comparison: number of significant and non-significant differences of hierarchically ordered models, respectively, vs. number of asexual waves per patient. The 40 patients with only one wave do not allow comparing  $M_2$  and  $M_1$  because the two models become identical. Numbers of patients with a given number of asexual waves are given in the bottom row*

Model Comparison	Significant difference	Number of asexual waves										$\Sigma$
		1	2	3	4	5	6	7	8	9	10	
$M_2$ vs. $M_1$	No	(40)	12	5	1	2	2	1	1	0	0	24 (+ 40)
	Yes	(0)	22	19	19	28	38	36	19	14	3	198
$T_1$ vs. $M_2$	No	14	17	15	12	15	23	17	14	5	1	133
	Yes	26	17	9	8	15	17	20	6	9	2	129
$T_2$ vs. $T_1$	No	32	24	21	13	20	22	23	11	9	1	176
	Yes	8	10	3	7	10	18	14	9	5	2	86
$W_1$ vs. $M_2$	No	31	21	19	12	24	34	20	11	7	1	180
	Yes	9	13	5	8	6	6	17	9	7	2	82
$W_2$ vs. $W_1$	No	34	24	18	13	23	24	24	12	11	3	186
	Yes	6	10	6	7	7	16	13	8	3	0	76
$G_1$ vs. $M_2$	No	31	21	19	12	24	34	20	11	7	1	180
	Yes	9	13	5	8	6	6	17	9	7	2	82
$G_2$ vs. $G_1$	No	31	23	16	10	23	20	20	11	9	2	165
	Yes	9	11	8	10	7	20	17	9	5	1	97
$\Sigma$		40	34	24	20	30	40	37	20	14	3	262

significantly better fits than  $M_2$ , whereby the proportion of improvements slightly increases with the number of asexual waves ( $p = 0.04$ ; logistic regression). For 97 patients, model  $G_2$  fits significantly better to the data than model  $G_1$ , again showing an increasing proportion of significant improvements if the number of waves per patient increases ( $p = 0.03$ ; logistic regression).

Summarizing, constant rates of gametocyte production  $\gamma$  and mortality  $\mu$  are not sufficient to reproduce the observed patterns of gametocytaemia. The use of wave-dependent transition rates and non-constant mortality as well as the incorporation of cytokine-mediated mortality lead to considerable successive improvements of the fits. The likelihood ratio tests of the three hierarchic branches of models indicate that, in general, either a time or an age dependency of the force of mortality is given. Within each branch, further improvements are made by adding cytokine-mediated mortality.

A score value is introduced to compare models which are not hierarchically connected, but have the same number of parameters (model groups

$T_1$ - $W_1$ - $G_1$  and  $T_2$ - $W_2$ - $G_2$ , respectively). For each patient, the likelihood values yielded by the three models are sorted in decreasing order and the models are given the scores 1, 2 and 3, respectively. The frequencies of the scores, reached by each model, are depicted in Table 3. In both model groups (with and without cytokine-mediated immunity), the models with Gompertz-type mortality yield the best scores. The Weibull-mortality models rank second whereas the models with time-dependent mortality are inferior. Pairwise sign tests confirm this ranking of models within each group ( $p < 0.001$ ).

The ranking of the three models of highest complexity  $T_2$ ,  $W_2$  and  $G_2$  is also visible in Figs 5(a)-(c). The main differences of the models lie in the reproduction of gametocytaemia dips and of the phases between consecutive waves of gametocytes. These features are best reproduced by the Gompertz model with cytokine-mediated mortality ( $G_2$ ). For a complete compilation of all 262 individual fits see our internet web page [http://www.uni-tuebingen.de/biometry/eu/eu\\_index.html](http://www.uni-tuebingen.de/biometry/eu/eu_index.html).

## 6. Discussion

Gametocytes have been used in intrahost models by Hellriegel (1992) and McKenzie & Bossert (1997, 1998), but these models lack verification by means of comparison with data. In Hellriegel's model, the rate of conversion of asexual parasites to gametocytes is constant (within a clone) and

TABLE 3

Model scores: for each patient, models with the same number of parameters are compared with each other: the fit with the highest likelihood scores 1, the fit with the lowest one scores 3

Model	Number of fits with score		
	1	2	3
$G_1$	128	108	26
$W_1$	65	172	25
$T_1$	32	61	169
$G_2$	147	87	28
$W_2$	53	179	30
$T_2$	31	62	169

sequestration is not taken into account. Gametocytes die at a basic rate, enhanced by immune effectors which interact with asexual parasites and gametocytes. McKenzie & Bossert (1997) investigate a system of three ordinary differential equations which describe asexual parasites, gametocytes and immune effectors. Concerning gametocytogenesis, they examine three cases: the number of gametocytes produced is proportional (i) to the asexual parasite density, or (ii) to the product of the asexual parasite density and the immune effector density, or (iii) to the square of the asexual parasite density. Sequestration of gametocytes is not explicit in the equations, but their display is delayed by ten days. According to their model, gametocytes die at a constant rate which is unaffected by immunity. Both Hellriegel and McKenzie & Bossert (1998) explore interactions between two parasite clones differing in their rates of gametocytogenesis.

According to our estimates, the transition rates  $\gamma$  vary considerably between different patients and between different asexual waves of the same

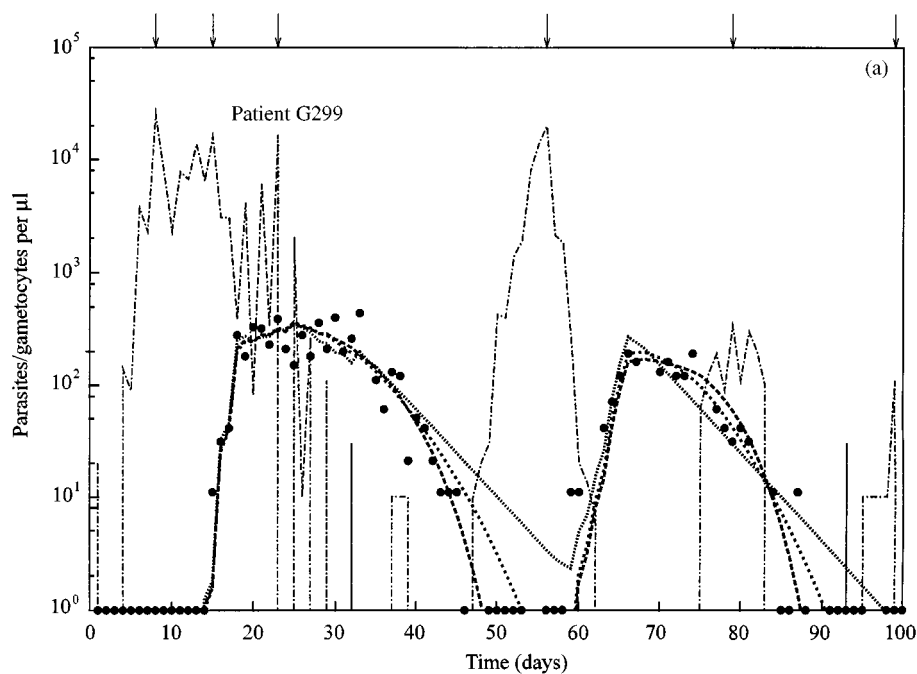


FIG. 5. Comparisons of the results of the three models of highest complexity ( $T_2$ ,  $W_2$  and  $G_2$ ; see Table 5 for parameter estimates). All models include cytokine-mediated mortality and different transition rates for each asexual wave.  $T_2$ : the base-line mortality rate grows linearly with time.  $W_2$ : the base-line mortality rate grows linearly with the age of the gametocytes (Weibull-type mortality).  $G_2$ : the base-line mortality rate grows exponentially with the age of the gametocytes (Gompertz-type mortality). (-----) asexual parasites; (●) observed gametocytes; (.....)  $T_2$ ; (— · — · —)  $W_2$ ; (— — —)  $G_2$ .

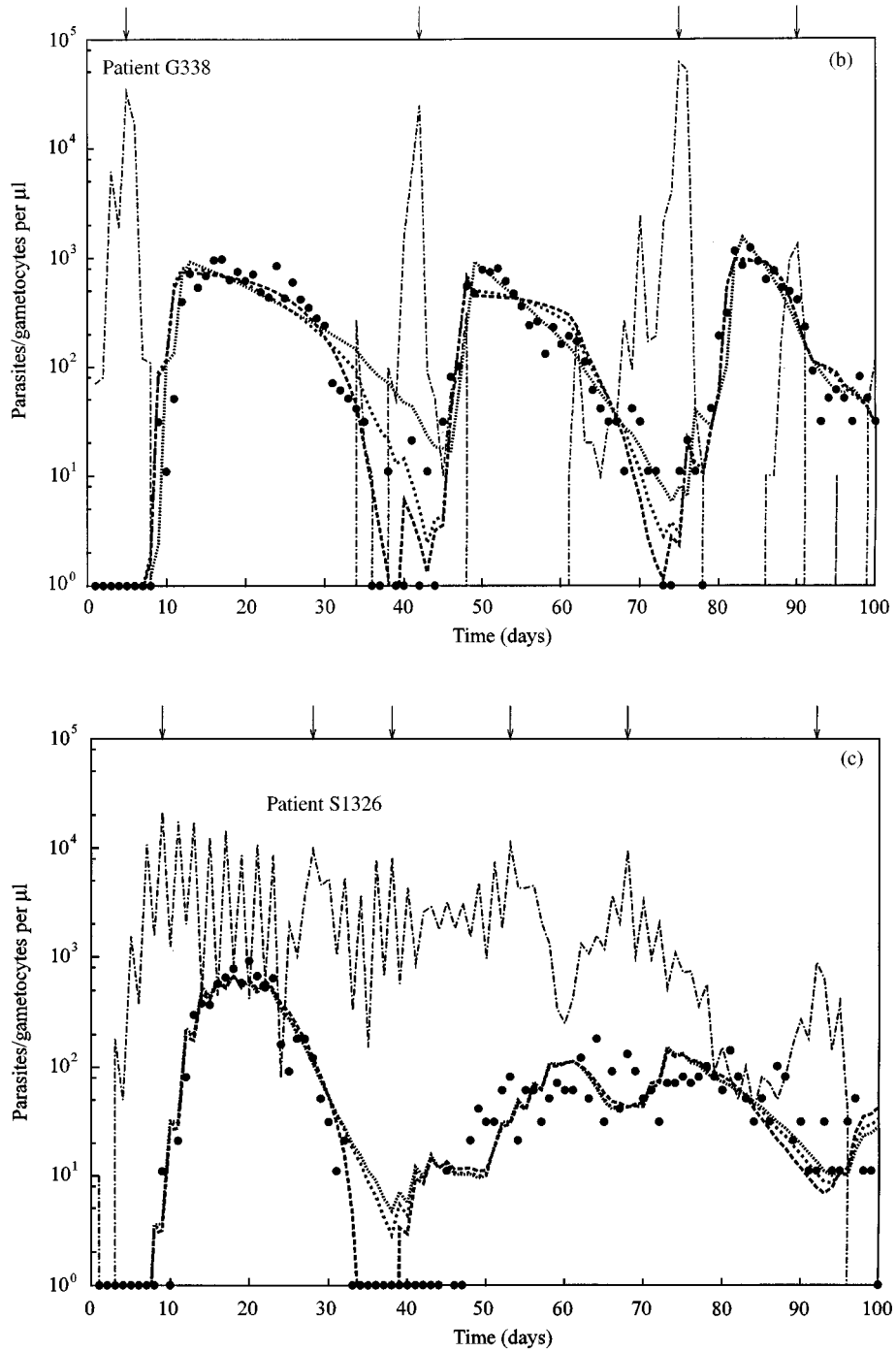


FIG. 5. (Continued).

patient: some asexual waves produce practically no gametocytes whereas, in the other extreme, practically all asexual parasites of a wave may contribute to gametocyte production. Some quantiles of  $\gamma$  are given in Table 4, together with those of the other parameters of  $G_2$  (a stratified

analysis of the estimated  $\gamma$ -values will be performed in a later publication).

The population median of the estimated gametocyte sequestration time  $D_s$  is seven days. Fifty percent of the  $D_s$  values range from 6 to 8 days (Table 4). The strongest information

TABLE 4  
*Quantiles of parameter estimates for model  $G_2$ : parameter values below the numerical precision (i.e.  $< 10^{-6}$ ) are set to zero*

Parameter	min	10%	25%	Median	75%	90%	max
$D_s$ (days)	1	4	6	7	8	9	33
$\gamma$ (days $^{-1}$ )	0	0	2.24E-4	3.44E-3	1.54E-2	5.18E-2	1.00
$\mu_0$ (days $^{-1}$ )	0	0	2.22E-4	3.00E-2	1.10E-1	2.34E-1	1.00
$\alpha_G$ (days $^{-1}$ )	0	0	4.50E-2	1.76E-1	7.39E-1	1.00	1.00
$\beta$ (days $^{-1}$ )	0	0	0	2.90E-3	1.88E-2	3.94E-4	1.00

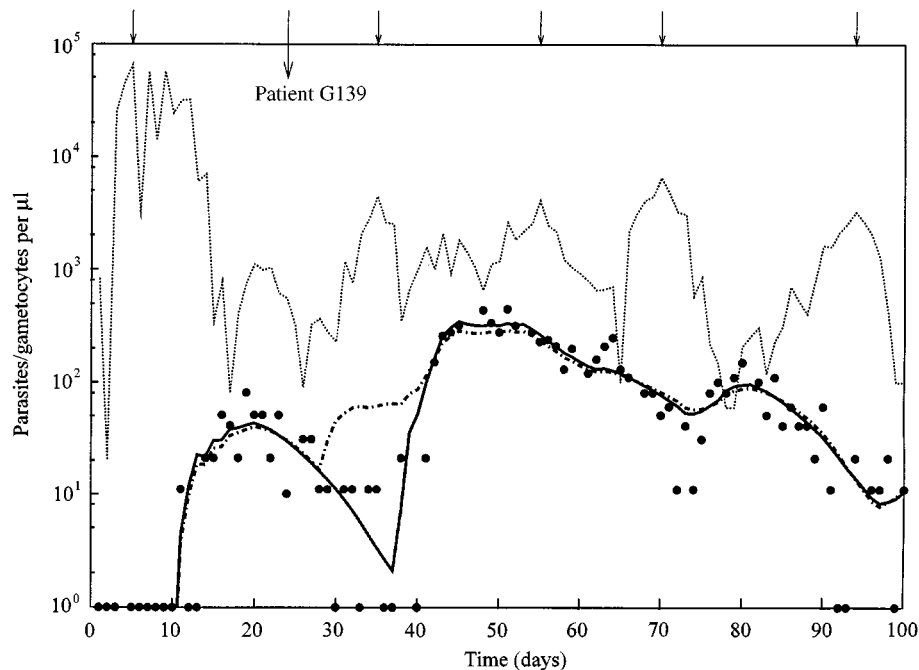


FIG. 6. An unsatisfactory fit (dotted line) which can be improved (full line) by assuming an additional asexual peak at day 24, contrary to the given rule (long arrow at the upper margin; see Table 5 for parameter estimates).  $G_2$ : the model assumes that mortality grows exponentially with the age of the gametocytes (Gompertz-type mortality) and is complemented by a cytokine-mediated mortality term; transition rates differ for each asexual wave. (.....) asexual parasites; (●) observed gametocytes; (.....)  $G_2$ ; (—) corrected.

on  $D_s$  comes from the time difference between the peak of the first asexual wave and the peak of the first wave of gametocytaemia. Estimation of the sequestration time may be biased because gametocytes were only likely to be observed if their density became larger than the detection level 10/ $\mu$ l of circulating blood. An initial wave of asexual parasitaemia with very low production rate (small  $\gamma$ ) may have produced so few gametocytes that none of them was observed by the microscopist. In such a case, estimation of  $D_s$  relies on matching subsequent asexual waves (which are much smaller than the initial one) with

subsequent gametocyte waves (which again are distorted by gametocyte mortality), so that—in case of a mismatch— $D_s$  may presumably be overestimated. In our models, we assume that for each patient the sequestration time is constant. Generally, a constant  $D_s$  yields satisfactory results, but for one patient (G161; Fig. 7) the sequestration time seems to change over time. Attempts to incorporate a changing  $D_s$  into the models failed because of lack of information in the data.

Some shapes of the Gompertz and Weibull-type survival functions are shown in Fig. 8 using

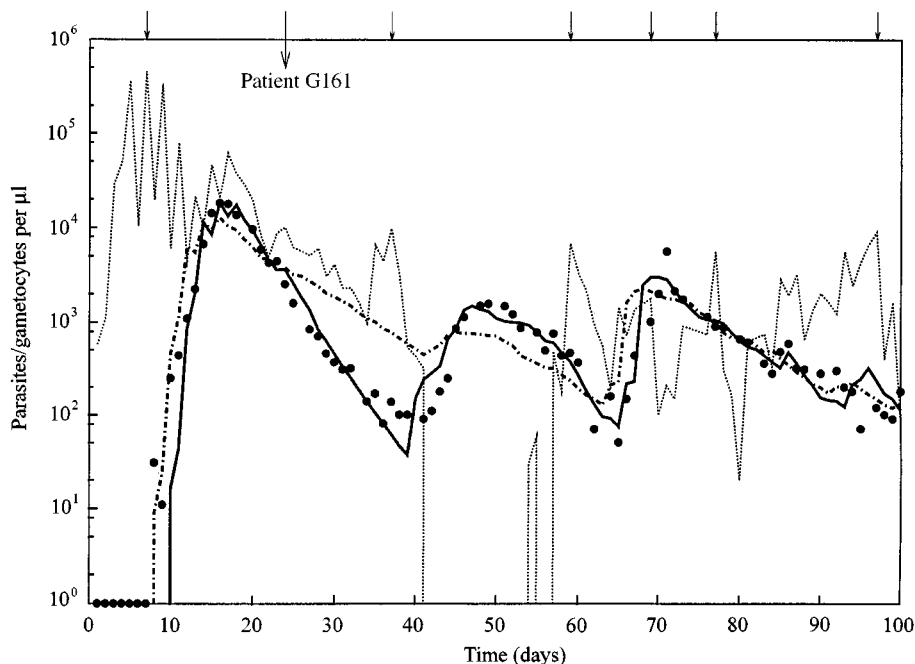


FIG. 7. An unsatisfactory fit (dotted line) which can be improved (full line) by assuming an additional asexual peak at day 24 (long arrow at the upper margin), contrary to the given rule, and by increasing the delay  $D_s$  by two days (see Table 5 for parameter estimates).  $G_2$ : the model assumes that mortality grows exponentially with the age of the gametocytes (Gompertz-type mortality) and is complemented by a cytokine-mediated mortality term; transition rates differ for each asexual wave. (.....) asexual parasites; (●) observed gametocytes; (.....)  $G_2$ ; (—) corrected.

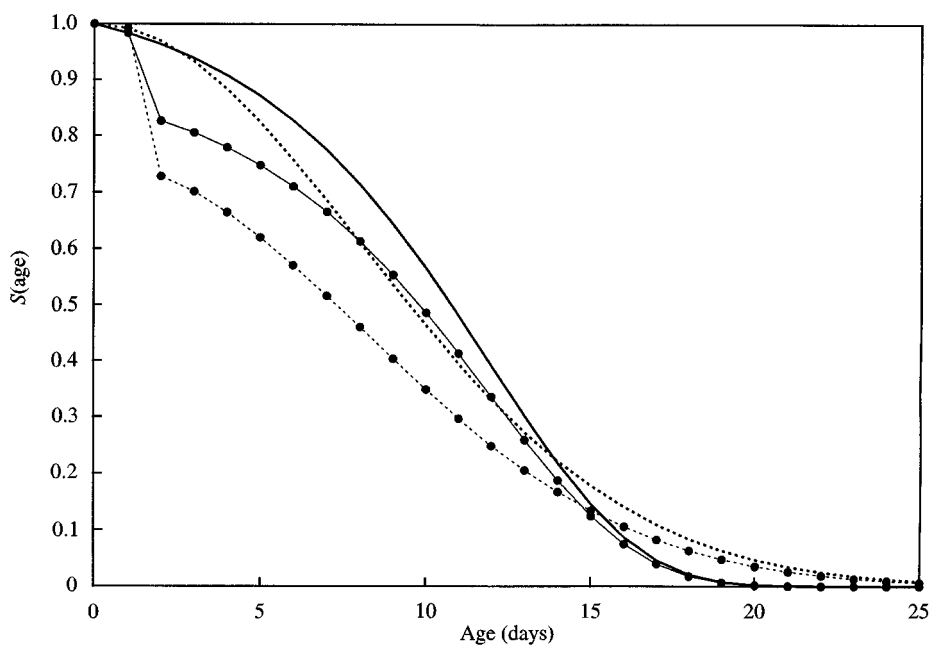


FIG. 8. Gametocyte survival functions corresponding to the linearly (—, denoted “ $W$ ” and “ $W + \text{toxin}$ ”) and exponentially (....., denoted “ $G$ ” and “ $G + \text{toxin}$ ”) increasing mortality, respectively. The parameter values are the estimates which were used in Fig. 3 (see Table 5). The curves without the dots show how gametocytes survive in the absence of asexual parasites, whereas the dotted curves assume a singular asexual peak of 500 000 parasites per  $\mu\text{l}$  at day 3. (—)  $G$ ; (.....)  $W$ ; (—●—)  $G + \text{toxin}$ ; (.....●.....)  $W + \text{toxin}$ .

TABLE 5

Parameter estimates of the examples presented in Figs 2–5: the first columns contain patient IDs and model identifiers; the suffix “-x” refers to the additionally defined asexual waves between  $\gamma_2$  and  $\gamma_3$  (see Figs 6–7 and text for details). The  $\alpha$ -column refers to either  $\alpha_T$ ,  $\alpha_W$  or  $\alpha_G$ , depending on the model. The units of the parameters are (days) for  $D_s$ , ( $\text{days}^{-2}$ ) for  $\alpha_T$  and  $\alpha_W$ , and ( $\text{days}^{-1}$ ) for the other parameters. Parameter values below the numerical precision (i.e.  $< 10^{-6}$ ) are set to zero

Patient	Model	$D_s$	$\mu_0$	$\alpha$	$\beta$	$\gamma_1$	$\gamma_2$	$\gamma_3$	$\gamma_4$	$\gamma_5$	$\gamma_6$	Figure	
S1300	$M_1$	7	1.88E-1	—	—	7.10E-2	—	—	—	—	—	2	
S1300	$M_2$	7	1.73E-1	—	—	1.73E-1	6.03E-3	1.73E-2	1.64E-2	0	—	2	
S1300	$T_1$	7	1.13E-1	2.94E-3	—	1.62E-1	8.95E-3	2.61E-2	4.60E-2	6.93E-2	—	2	
S1300	$T_2$	7	1.17E-1	0	5.62E-2	1.43E-1	1.94E-2	3.01E-2	3.39E-2	6.38E-2	—	2	
G305	$M_1$	7	1.62E-1	—	—	4.54E-2	—	—	—	—	—	3	
G305	$M_2$	6	1.30E-1	—	—	1.40E-1	3.67E-2	7.68E-3	0	0	—	3	
G305	$W_1$	6	0	1.82E-2	—	1.10E-1	3.66E-2	6.71E-3	4.88E-4	0	—	3	
G305	$W_2$	6	0	1.54E-2	2.17E-2	1.05E-1	3.88E-2	1.27E-2	1.91E-3	3.81E-4	—	3 + 8	
G305	$G_2$	6	0.15E-1	2.30E-1	1.16E-2	9.91E-2	3.56E-2	9.39E-3	1.13E-3	2.05E-4	—	3 + 8	
G104	$M_2$	7	1.40E-1	—	—	3.15E-2	—	—	—	—	—	4	
G104	$M_2$	7	1.19E-1	—	—	4.10E-2	8.56E-3	0	0	2.16E-3	1.76E-2	4	
G104	$G_1$	7	6.45E-2	5.96E-2	—	3.55E-2	9.44E-3	3.05E-3	2.27E-3	6.70E-3	1.45E-2	4	
G104	$G_2$	7	5.34E-2	5.89E-2	4.74E-2	3.25E-2	2.58E-2	2.66E-2	1.03E-2	1.22E-2	4.45E-2	4	
G299	$T_2$	10	1.81E-1	0	0	8.34E-3	6.82E-3	3.98E-3	6.88E-3	0	4.31	5(a)	
G299	$W_2$	10	0	1.67E-2	4.43E-3	6.47E-3	4.35E-3	8.49E-4	4.24E-3	0	0	5(a)	
G299	$G_2$	10	1.27E-2	2.00E-1	9.62E-3	6.94E-3	3.92E-3	0	3.59E-3	0	1.70E-4	5(a)	
G338	$T_2$	7	4.01E-2	2.04E-3	2.18E-2	1.72E-2	3.04E-2	1.46E-2	1.37E-2	—	—	5(b)	
G338	$W_2$	6	0	8.36E-3	5.81E-2	1.43E-2	2.32E-2	8.20E-3	0	—	—	5(b)	
G338	$G_2$	6	8.42E-3	1.80E-1	6.44E-2	1.31E-2	2.21E-2	8.07E-3	0	—	—	5(b)	
S1326	$T_2$	5	0	0	4.11E-2	1.91E-2	0	1.03E-3	5.87E-3	1.03E-2	9.51E-3	5(c)	
S1326	$W_2$	5	2.69E-5	8.85E-3	3.36E-2	1.77E-2	0	9.87E-4	5.44E-3	9.83E-3	1.28E-2	5(c)	
S1326	$G_2$	5	2.90E-5	1.00	2.83E-2	1.56E-2	0	9.10E-4	4.79E-3	8.72E-3	1.61E-2	5(c)	
G139	$G_2$	8	2.02E-2	2.08E-1	0	1.37E-4	1.74E-2	4.73E-3	2.86E-3	1.27E-3	—	6	
G139	$G_{2-x}$	8	5.06E-2	1.26E-1	0	1.71E-4	2.97E-4	2.44E-2	5.27E-3	3.45E-3	1.21E-3	—	6
G161	$G_2$	7	4.25E-2	0	2.13E-1	1.53E-2	1.95E-2	2.10E-1	1.14E-1	2.14E-2	5.79E-3	7	
G161	$G_{2-x}$	9	5.94E-2	0	3.58E-2	2.78E-2	9.94E-4	5.36E-2	3.33E-1	1.43E-1	4.53E-2	1.12E-2	7

parameter estimates of  $W_2$  and  $G_2$  for patient G305 (cf. Fig. 3). Undisturbed gametocyte survival in the absence of asexual parasites is depicted with bold curves. The dotted curves show how survival decreases on day 3 because of cytokine-mediated mortality, caused by a large singular peak of 500 000 asexual parasites per  $\mu\text{l}$ . The choice of the expression  $\beta \log_{10}(A(t) + 1)$  to model cytokine-mediated mortality is somewhat arbitrary and may be regarded as an experimental feature which allows to incorporate additional mortality, caused by high asexual stage densities. Although the fits of models  $G_i$  and  $W_i$  ( $i = 1, 2$ ) seem to differ only slightly [Figs 5(a)–(c)], epidemiological implications can depend crucially on the shapes of the gametocyte survival functions.

Our parameter estimation leads to a few unacceptable fits, two of which are depicted in Figs. 6 and 7 (dashed graphs). Patient G139 (Fig. 6) may have an additional wave of asexual parasites, caused by a different  $Pf_{\text{emp1}}$ -variant, between days 15 and 30, which is not recognized as separate wave by our definition. Assuming an additional peak on day 24, one more  $\gamma$ -value needs to be estimated and the resulting fit becomes much more acceptable (Fig. 6). A similar problem occurs with patient G161 (Fig. 7): inserting an additional peak on day 24 and increasing the delay  $D_s$  by two days improve the fit considerably. The additional delay of two days leads to a bias at the beginning of the curve but improves the fit for the remainder of the curve considerably.

To conclude, we found that the gametocyte sequestration time lasts about one week. Estimates of the transition rates of asexual parasites to gametocytes,  $\gamma$ , change considerably among different waves of asexual parasites of each patient. Gametocyte survival can best be modelled by using an age-dependent Gompertz-type mortality. There is also strong evidence that high parasite densities increase the mortality of gametocytes, supporting the hypothesis of cytokine-mediated mortality. This shows that the dynamics

of gametocytogenesis and gametocytaemia are much more complicated than assumed in previously published models.

Support by the European commission is acknowledged (Project No. IC18CT97-0242). We thank the participants of the Concerted Action "Mathematical models of the immunological and clinical epidemiology of *P. falciparum* malaria" for helpful discussions. We also thank Adrian Luty for his help with improving our English.

#### REFERENCES

- BAIRD, J. K., JONES, T. R., PURNOMO, MASBAR, S., RATIWAYANTO, S. & LEKSANA, B. (1991). *Am. J. Trop. Med.* **44**, 183.
- BORST, P., BITTER, W., MCCULLOCH, R., VANLEEUEWEN, F. & RUDENKO, G. (1995). *Cell* **82**, 1.
- BRUCE, M. C., ALANO, P., DUTHIE, S. & CARTER, R. (1990). *Parasitology* **100**, 191.
- CARTER, R. & GRAVES, P. (1988). In: *Malaria—Principles and Practice of Malariology* (Wernsdorfer, W. H. & McGregor, I. eds), Vol. 1, pp. 253–305. London: Livingstone.
- CARTER, R. & MILLER, L. H. (1979). *Bull. WHO* **57** (Suppl. 1), 37.
- DAY, K. P., HAYWARD, R. E. & DYER, M. (1998). *Parasitology* **116**, 95.
- EARLE, W. C. & PEREZ, M. (1932). *J. Lab. Clin. Med.* **17**, 1124.
- EYLES, D. E. & YOUNG, M. D. (1951). *J. Nat. Malaria Soc.* **10**, 327.
- GARNHAM, P. C. C. (1998). In: *Malaria—Principles and Practice of Malriology* (Wernsdorfer, W. H. and McGregor, I. eds), Vol. 1, pp. 61–96. London: Churchill Livingstone.
- HELLRIEGEL, B. (1992). *Proc. Roy. Soc. London B* **250**, 249.
- JEFFERY, G. M. (1960). *Am. J. Trop. Med. Hyg.* **9**, 315.
- JEFFERY, G. M. & EYLES, D. E. (1954). *Am. J. Trop. Med. Hyg.* **2**, 219.
- KARUNAWEEERA, N. D., CARTER, R., GRAU, G. E., KWIATKOWSKI, D., DEL GIUDICE, G. & MENDIS, K. N. (1992). *Clin. Exp. Immunol.* **88**, 499.
- MCKENZIE, F. E. & BOSSERT, W. H. (1997). *J. theor. Biol.* **188**, 127.
- MCKENZIE, F. E. & BOSSERT, W. H. (1998). *J. theor. Biol.* **193**, 419.
- NAOTUNNE, T. S., KARUNAWEEERA, N. D., DEL GIUDICE, G., KULARATNE, M. U., GRAU, G. E., CARTER, R. & MENDIS, K. N. (1991). *J. Exp. Med.* **173**, 523.
- NAOTUNNE, T. S., KARUNAWEEERA, N. D., MENDIS, K. N. & CARTER, R. (1993). *Immunology* **78**, 555.
- SMALLEY, M. E. & BROWN, J. (1981). *Trans. Roy. Soc. Trop. Med. Hyg.* **75**, 316.